

## Evidence against Focused Chains in High-Yield Copper Sputtering\*

N. THOMAS OLSON AND HAROLD P. SMITH, JR.

*Space Sciences Laboratory, University of California, Berkeley, California*

(Received 5 October 1966; revised manuscript received 14 December 1966)

The yield (atoms/ion) and angular distribution (atoms/ion sr) of monocrystalline copper sputtered by 1- to 10-keV cesium ions has been measured as a function of target temperature at normal and at 45° incidence to the (100) face. The yield as a function of energy and at normal incidence attained a broad maximum of 6.2 atoms/ion in the neighborhood of 5 keV and was independent of target temperature variation from 77 to 493°K. At non-normal incidence, the sputtering yield was markedly affected by the opacity of the target lattice to the incident ion beam, as is demonstrated by a higher yield for incidence along the [755] direction when compared with the [110] direction. The fitting of an analytic function to the extensive angular emission data by nonlinear regression analysis indicated that preferred emission along the close-packed direction was of secondary importance, decreasing from 18% at 1 keV to 10% at 10 keV. The primary contribution to the sputtering distribution followed a polar angle cosine dependence.

### INTRODUCTION

**E**XTENSIVE computer simulation of the  $n$ -body interactions of radiation damage<sup>1-3</sup> and sputtering<sup>4-6</sup> have offered new insight into the mechanisms of these processes. At least two aspects of the apparent mechanisms merit further quantitative experimentation. (a) Long chains of focused collisions, as proposed by Silsbee,<sup>7</sup> are evident in radiation-damage simulation but are absent in sputtering simulation. The presence of a surface and extensive interaction by the primary in the latter case are the probable reasons for the absence. (b) The number of sputtered particles per ion is reduced by the penetration of the primary particle into the lattice.

A radioactive tracer technique, previously described,<sup>8</sup> offers a sensitive, quantitative measurement of the yield (atoms/ion) and angular distribution (atoms/ion sr). Comparison of these results with similar and voluminous data available through simulation should provide experimental verification of the computer results noted above. In particular, the measurements presented are for 1- to 10-keV cesium-ion (Cs<sup>+</sup>) bombardment of the (100) face of copper at normal incidence and at 45° incidence with three target temperatures of 77, 293, and 473°K.

\* Work supported by the Lewis Research Center of the National Aeronautics and Space Administration.

<sup>1</sup> J. B. Gibson, A. N. Goland, M. Milgram, and G. H. Vineyard, *Phys. Rev.* **120**, 1229 (1960).

<sup>2</sup> C. Erginsoy, G. H. Vineyard, and A. Englert, *Phys. Rev.* **133**, A595 (1964).

<sup>3</sup> C. Erginsoy, G. H. Vineyard, and A. Shimizu, *Phys. Rev.* **139**, A118 (1965).

<sup>4</sup> W. L. Gay and D. E. Harrison, Jr., *Phys. Rev.* **135**, A1780 (1964).

<sup>5</sup> D. E. Harrison, Jr., J. P. Johnson, III, and N. S. Levy, *Appl. Phys. Letters* **8**, 33 (1966).

<sup>6</sup> H. J. Amster and R. N. Schlaug [R. N. Schlaug, Ph.D. thesis, Department of Nuclear Engineering, University of California, Berkeley, 1965 (unpublished)].

<sup>7</sup> R. H. Silsbee, *J. Appl. Phys.* **28**, 1246 (1957).

<sup>8</sup> N. T. Olson and H. P. Smith, Jr., *Am. Inst. Aeron. Astronaut. J.* **4**, 916 (1966).

### EXPERIMENTAL TECHNIQUE AND INSTRUMENTATION

The experimental apparatus, described previously,<sup>8</sup> consisted primarily of a cesium contact ionization source, radioactive monocrystalline copper target, and separable collector assembly. The ion source and target vacuum chambers were differentially pumped to operating pressures less than  $1.5 \times 10^{-7}$  Torr. The target current density varied from 14 to 28  $\mu\text{A}/\text{cm}^2$ , depending on the ion energy, so that the rate of arrival of residual background gas was a factor of 10 less than the rate of removal of sputtered copper atoms.

The radioactive monocrystalline target, mounted in the collector assembly as illustrated in Fig. 1, was aligned to within 1° of the [100] crystallographic direction at normal incidence and the [110] or [755] at 45° incidence. The radioactivity was induced by exposing the copper target to a thermal neutron flux of  $5 \times 10^{12}$  neutrons  $\text{cm}^{-2} \text{sec}^{-1}$  for 15 min, thus providing sufficient activity to detect 0.1  $\mu\text{g}$  of sputtered copper when measured using a NaI scintillation well crystal with multichannel spectrum analysis.

The collector, also illustrated in Fig. 1, surrounded the entire  $2\pi$  sr above the target so that both angular and total yield measurements were possible. To facilitate the angular distribution measurements, 2.7 sr of the collector above the target were fabricated from 100 aluminum cubes placed in a  $10 \times 10$  array. The polar and azimuthal positions of the 25 collectors in each quadrant are given in Fig. 2 along with their solid angle relative to the target. The angular distribution was determined by measuring the copper radioactivity of each cube. An absolute measure was then obtained by direct comparison with the radioactivity of a copper standard of known weight irradiated at the same time and under the same conditions as the target. The sides and top portions of the collector were aluminum foil which was folded into a cube for counting. Thus, the total yield was determined by summing the amount of

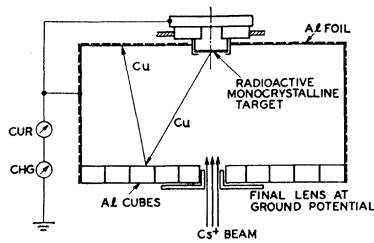


FIG. 1. Schematic diagram of target-collector assembly for measurement of the yield and angular distribution of sputtered copper. Secondary sputtering of previously collected copper is depicted.

copper on the 100 cubes, the side, and top foils. In principle, the top collector foil, residing in the plane of the target surface, should not have collected any sputtered copper. It did, however, collect 2 to 3% of the total. This fraction (as illustrated in Fig. 1) could be a result of secondary sputtering of copper already collected on the cubes or a sticking probability slightly less than unity. Whichever the case, the error in the measured distribution is small.

The total number of ions striking the target was determined by summing and integrating the current to the target and collector assembly which served as a simplified Faraday cage. Since none of the ion beam struck the collector, this method eliminated any inaccuracy associated with secondary and photoelectron production at the target.

## RESULTS AND DISCUSSION

### 1. Total Yield

The total yield,  $S(E, T, \alpha)$ , shown in Figs. 3 and 4, as a function of ion energy  $E$ , target temperature  $T$ , and angle of incidence  $\alpha$ , measured from the surface normal, emphasizes the importance of heavy ion "chan-

posn	1	2	3	4	5
$\theta$ ( $^\circ$ )	50	51	53	56	59
$\phi$ ( $^\circ$ )	83	71	61	52	45
$\Delta\Omega$ (sr)	.018	.016	.014	.012	.009
6	7	8	9	10	
$\theta$ ( $^\circ$ )	42	44	48	52	56
$\phi$ ( $^\circ$ )	82	66	54	45	38
$\Delta\Omega$ (sr)	.027	.024	.020	.015	.012
11	12	13	14	15	
$\theta$ ( $^\circ$ )	33	37	42	48	53
$\phi$ ( $^\circ$ )	78	59	45	36	29
$\Delta\Omega$ (sr)	.039	.034	.027	.020	.014
16	17	18	19	20	
$\theta$ ( $^\circ$ )	22	29	37	44	51
$\phi$ ( $^\circ$ )	71	45	31	24	19
$\Delta\Omega$ (sr)	.053	.045	.034	.024	.016
21	22	23	24	25	
$\theta$ ( $^\circ$ )	10	22	33	42	50
$\phi$ ( $^\circ$ )	45	19	12	8	7
$\Delta\Omega$ (sr)	.064	.053	.039	.027	.018

FIG. 2. Schematic diagram of the angular collector positions for normal bombardment of the (100) surface.  $\theta$  is the polar angle taken equal to zero along the target surface normal while  $\phi$  is the azimuthal angle measured as shown in the surface plane. The solid angle in steradians is presented for each collector position.

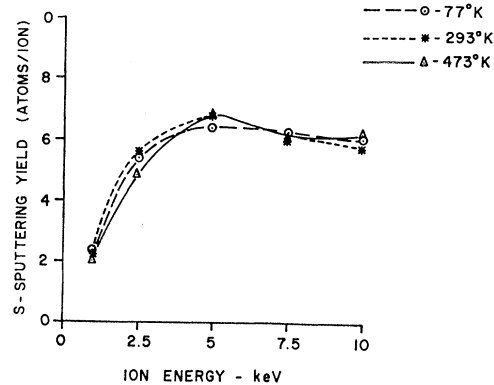


FIG. 3. Sputtering yield versus incident ion energy for 1- to 10-keV cesium-ion bombardment of monocrystalline copper at 77, 293, and 473°K. The ion beam was normal to the surface and parallel to the [100] direction.

neling"<sup>9,10</sup> in the sputtering process. Ions, incident along the open or transparent [100] axis, as was the case for the normal-incidence experiments, have a smaller probability of losing energy by momentum transfer to lattice atoms in the first few monolayers than those ions directed along randomly oriented crystallographic axes. Therefore, the sputtering yield for ion beam alignment parallel to low-index directions should be less than the yield encountered in sputtering of polycrystalline targets under the same experimental conditions. Furthermore, the yield as a function of incident ion energy is expected to reach a maximum and to decrease as the energy of the ion is increased since the effective radius of interaction for momentum transfer to the lattice atoms also decreases, thus enhancing the channeling process and reducing the magnitude of the total yield. Alignment of the ion beam with those

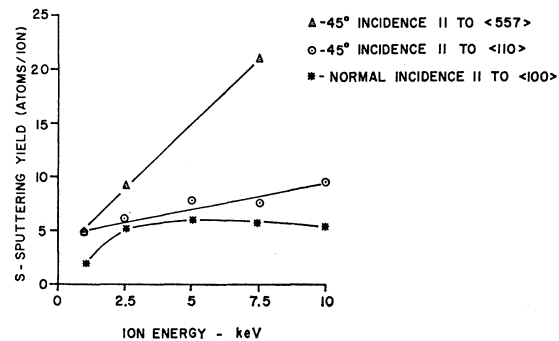


FIG. 4. Energy dependence of the total sputtering yield for ion beam incident at 45° to the target normal and parallel to the [110] and [755] crystallographic directions. The yield at normal incidence and 293°K has been included for comparison.

<sup>9</sup> E. V. Kornelson, F. Brown, J. Davies, B. Domeij, and G. Piercy, Phys. Rev. **136**, A849 (1964).

<sup>10</sup> T. S. Noggle and O. S. Oen, Phys. Rev. Letters **10**, 395 (1966).

crystallographic directions that enhance channeling should then reduce the energy at which the maximum occurs.

Comparison of the data presented in Fig. 3 with those of Almen and Bruce,<sup>11</sup> who report a xenon-polycrystalline copper yield of 10 atoms per ion at 10 keV, whereas we report 6, substantiates the contention of reduced yield for low-index alignment. The same reference also shows that  $(\partial S/\partial E)_{E=10 \text{ keV}} > 0$  for a polycrystalline target, whereas a broad plateau,  $(\partial S/\partial E)_{E>5 \text{ keV}} \approx 0$  can be discerned in our mono-crystalline copper yield curve of Fig. 3.<sup>12</sup>

Similar conclusions can be drawn with regard to measurements at  $\alpha=45^\circ$ . Since non-normal incidence decreases ion penetration normal to the surface of the lattice without significantly affecting total momentum transfer per collision, the  $S(E)$  curve at  $\alpha=45^\circ$  is expected to be higher than that at  $0^\circ$ , as is the case shown in Fig. 4.<sup>13</sup> The effect of ion penetration is further emphasized by the large increase in yield for bombardment along the opaque [755] as opposed to the transparent [110] direction. The high-yield, high-index results are similar to the data of Magnuson *et al.*,<sup>14</sup> who report a monotonically increasing  $S(E)$  curve for argon-ion bombardment of the (110) face of copper parallel to the [111] direction, which is relatively opaque in the fcc system despite the low value of the Miller indices.

Target temperature variation from 77 to 473°K had no measurable effect on total yield. If it is contended that the primary effect of target temperature on sputtering is annealing of the ion-bombardment-induced radiation damage,<sup>15</sup> then the effect of the above temperature variation should be small since radiation damage studies indicate that rapid annealing occurs in copper for temperature greater than 100°K.<sup>16,17</sup>

## 2. Angular Distribution Measured at Normal Incidence

The angular distribution is reported as the fractional yield per unit fractional solid angle,

<sup>11</sup> O. Almen and G. Bruce, Nucl. Instr. Methods **11**, 279 (1961).  
<sup>12</sup> Similar results can be noted in argon-copper sputtering: J. M. Fluit, J. Kistemaker, and C. Snoek, Physica **30**, 870 (1964); T. W. Snouse and L. C. Haughney, J. Appl. Phys. **37**, 700 (1966); A. L. Southern, W. R. Willis, and M. T. Robinson, *ibid.* **34**, 153 (1963).

<sup>13</sup> Snouse has compiled a considerable amount of data taken at  $\alpha=0$ , demonstrating that the Cu yield for bombardment along the [100] direction exceeds that along the [110] direction over a wide range of  $E$ . Hence, our data emphasized the importance of reducing the effective penetration (i.e., oblique incidence) since the yields of the two crystallographic directions are reversed by bombarding the [100] direction at  $\alpha=0$  and the [110] direction at  $\alpha=45^\circ$ .

<sup>14</sup> G. D. Magnuson and C. E. Carlston, J. Appl. Phys. **34**, 3267 (1963).

<sup>15</sup> J. B. Green, N. Thomas Olson, and H. P. Smith, Jr., J. Appl. Phys. **37**, 4699 (1966).

<sup>16</sup> E. P. Cooper and M. M. Mills, North American Aviation Report No. SR-78, 1950 (unpublished).

<sup>17</sup> R. R. Coltman, T. H. Blewitt, C. E. Klabunde, and J. K. Redman, Bull. Am. Phys. Soc. **4**, 235 (1959).

$(\Delta S_i/S)/(\Delta\Omega_i/2\pi)$ , where  $\Delta S_i$  is the yield on and  $\Delta\Omega_i$  is the solid angle subtended by the  $i$ th collector. A nonlinear regression analysis of the 100, fourfold symmetric, angular data points, normalized to isotropic emission, was made in order to express the data in analytic form.

$$\frac{2\pi}{S} \frac{dS}{d\Omega}(\theta, \phi) = B_1 \cos\theta + B_2 \times \exp\{-(2\sigma^2)^{-1}[(\theta_1 - \theta)^2 + (\phi_1 - \phi)^2 \sin^2\theta_1]\}, \quad (1)$$

where

$$S = \int_{2\pi} d\Omega(\theta, \phi) (dS/d\Omega)(\theta, \phi),$$

and  $\theta$  and  $\phi$  are, respectively, the polar and azimuthal angles. The values of  $\theta_1$  and  $\phi_1$  were determined by the orientation of the [110] crystallographic direction with respect to the collector, while  $B_1$ ,  $B_2$ , and  $\sigma$  were adjusted by regression analysis to yield minimum (square) error between the analytic function and the 100 data. A second regression analysis, in which  $\theta_1$  and  $\phi_1$  were adjusted rather than predetermined by the [110] orientation, had no significant effect.

The Gaussian functions, centered about the close-packed directions, were chosen for their convenience in representing "Wehner spots"<sup>18</sup> and because of the similarity of the function to the sputtering angular emission data of Nelson, Thompson, and Montgomery.<sup>19</sup> The cosine distribution, centered about the surface normal, was chosen to represent the monotonically decreasing emission with increasing polar angle. Such a distribution would be a result of uniform isotropic scattering from random centers in the target volume. Representation of preferred emission in the [100] direction by a Gaussian was not fruitful since the planar angular resolution of the collectors in this direction exceeds  $10^\circ$ , and the beam entrant hole prevented sputtered particle collection at the point of maximum emission in these particular measurements. (See Fig. 2.)

The accuracy of the proposed emission representation can be judged by the 14% or less average absolute percent deviation of the 100 data, whose accuracy is of the order of 10%, utilizing only three fitting parameters. In addition, integration of  $(1/S)dS/d\Omega$  over the  $2\pi$  sr above the target should give unity.

$$\frac{4}{S} \int_0^{\pi/2} d\phi \int_0^{\pi/2} d\theta \sin\theta \frac{dS}{d\Omega}(\theta, \phi) = \frac{1}{2}B_1 + 4B_2\sigma^2 \equiv 1. \quad (2)$$

This condition of conservation of particles is met to within 11% using the values of  $B_1$ ,  $B_2$ , and  $\sigma$  obtained from regression analysis. The integration also provides

<sup>18</sup> G. K. Wehner, Advan. Electron. Electron Phys. **7**, 239 (1955).

<sup>19</sup> R. S. Nelson, M. W. Thompson, and H. Montgomery, Phil. Mag. **7**, 1385 (1962).

TABLE I. Tabulated values of adjustable constants in Eq. (1) as a function of incident ion energy and target temperature. It should be noted that  $\frac{1}{2}B_1$  is the relative emission in a cosine distribution while  $4B_2\sigma^2$  is the relative emission in the preferred, close-packed directions.

Ion energy (keV)	Target temperature ( $^{\circ}$ K)	Total yield (atoms/ion)	$\frac{1}{2}B_1$	$4B_2\sigma^2$	$\frac{1}{2}B_1+4B_2\sigma^2$	$\sigma$ (deg)
1	77	2.2	0.77	0.17	0.94	9.2
2.5	77	5.4	0.83	0.13	0.96	8.0
5	77	6.3	0.88	0.14	1.02	8.1
7.5	77	6.2	0.94	0.12	1.06	7.1
10	77	6.0	0.91	0.13	1.04	7.1
1	293	2.1	0.75	0.17	0.92	9.7
2.5	293	5.6	0.78	0.16	0.94	9.6
5	293	6.7	0.92	0.11	1.03	6.7
7.5	293	5.9	0.91	0.11	1.02	7.1
10	293	5.7	0.89	0.09	0.98	7.1
1	473	2.1	0.74	0.18	1.02	9.4
2.5	473	4.8	0.92	0.13	1.05	8.5
5	473	6.8	1.00	0.11	1.11	7.8
7.5	473	6.0	0.95	0.11	1.06	8.0
10	473	6.2	0.99	0.10	1.09	7.7

the relative contributions of the cosine ( $\frac{1}{2}B_1$ ) and Gaussian ( $4B_2\sigma^2$ ) emissions. The quantities  $\frac{1}{2}B_1$ ,  $4B_2\sigma^2$ ,  $\frac{1}{2}B_1+4B_2\sigma^2$ , and  $\sigma$ , as well as the measured yield  $S$  are shown in Table I.

Three features of the analysis are noted: (a) The Gaussian distribution accounts for 18% or less of the emitted particles, thereby demonstrating the second-order effect of preferred emission at high yield along the close-packed directions. Furthermore, the relative contribution of Gaussian emission decreases with increased ion energy. Obviously, cosine emission is the major sputtering mechanism. (b) There is, again, no significant dependence upon temperature. (c) The angular width of Gaussian emission is comparable to the collector angular resolution, thereby vitiating interpretation of this variable and suggesting improved resolution in future measurements.

These experimental results suggest that in the region of normal incidence and high yield, focused chains, if

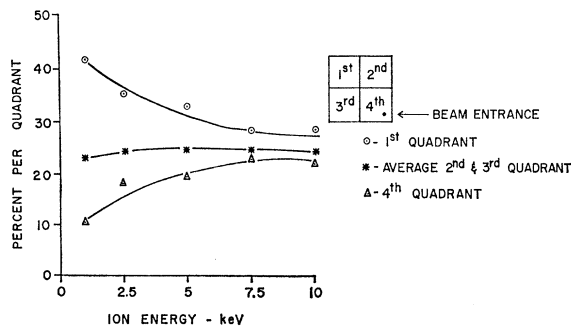


FIG. 5. Percent yield per collector quadrant for the ion beam incident  $45^{\circ}$  to the target surface and parallel to the  $[110]$  crystallographic direction. The ion beam entered the target-collector chamber along the diagonal of the fourth quadrant as shown in the insert.

present, are of secondary importance. It should be noted that the small amount of preferred emission in the close-packed direction could be attributed to two or three (noncollinear) collisions as discussed by Harrison *et al.*<sup>5</sup>

### 3. Angular Distribution Measured at Non-Normal Incidence

Lack of azimuthal symmetry, inherent at  $\alpha=45^{\circ}$ , precluded convenient nonlinear regression analysis of the angular distribution measurements. Certain qualitative aspects, however, were apparent in the data. The distribution again was characterized by preferred emission along the four  $\langle 110 \rangle$  directions superimposed upon a background distribution skewed in the direction away from the incident beam. As noted at normal incidence, the preferred emission was of secondary importance.

Further qualitative features are evident in Figs. 5 and 6, in which the percent collection in each quadrant of the fourfold symmetric collector is plotted as a

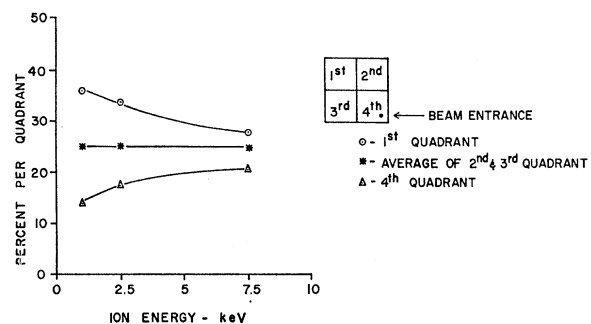


FIG. 6. Percent yield per collector quadrant for the ion beam incident  $45^{\circ}$  to the target surface and parallel to the  $[755]$  crystallographic direction.

function of energy. The effect of tilting the ion beam away from normal incidence, evidently, is more important at the lower range of energy than at the higher. This is attributed to increased penetration at higher energy. Under this condition, it can be conjectured that the initial momentum of the ion is dissipated throughout a larger lattice volume with the resultant distribution approaching that for normal incidence. Again, the importance of the depth of the collision below the surface is thought to be a primary factor in the emission of sputtered particles, whereas focused collision transport to the surface is thought to be a secondary consideration.

### CONCLUSIONS

From the measured data, it is apparent that the sputtering yield and angular distribution can be markedly affected by the crystalline state of the target and

its orientation relative to the incident ion beam. The yield is low for incidence along open crystallographic directions such as the [110] or [100] axis while it is increased quite substantially for incidence along the opaque [755] direction. The maximum in the yield as a function of ion energy has been noted in many experiments and has been attributed to the competition between higher-energy transfer to lattice particles and increased penetration of the incident particle as the energy is increased.

The angular distribution results, as interpreted by the nonlinear regression analysis fit of Eq. (1) to the data, suggest that the close-packed focusing contribution to sputtering in these measurements is a second-order effect. The major contribution (80% or more) is a result of the cosine term of Eq. (1) which could be representative of random scattering within the crystal lattice.

## Magnetic Resonance in Single-Crystal Terbium Metal at 100 GHz\*

JOHN L. STANFORD AND ROBERT C. YOUNG†

*Institute for Atomic Research and Department of Physics, Iowa State University, Ames, Iowa*

(Received 10 November 1966; revised manuscript received 9 January 1967)

The absorption of 100-GHz (3-mm) microwave radiation has been studied as a function of temperature and applied magnetic field in single-crystal terbium metal. For magnetic fields up to 26 kOe, three main features are observed in the absorption spectrum: (a) an absorption onset occurring at low fields and low temperatures, which is shown to be associated with the effects of domain rotation; (b) an absorption line occurring around 19 kOe. This line is essentially temperature-independent, although it greatly intensifies below the Curie temperature  $T_C$ ; (c) a temperature-dependent absorption line which exhibits a dramatic shift as the sample is cooled through  $T_C$ , even in the presence of fields thought to be sufficiently strong to destroy the antiferromagnetic ordering and induce ferromagnetic alignment above  $T_C$ . The resonance line-widths are very large ( $\sim 5$  to 10 kOe). At low temperatures this line is in good agreement with the theory of Cooper and Elliott for ferromagnetic resonance in a material with large twofold magnetic anisotropy. Extrapolation to  $T=0$  yields a value of the twofold-anisotropy constant  $K_2$  for terbium of  $5.3 \times 10^8$  erg/cm<sup>3</sup>  $\pm 7\%$ . This is in excellent agreement with the latest static-torque data of Rhyne and Clark for terbium, substantiating their result as well as reducing the uncertainty involved in their technique by more than a factor of 3. The agreement with theory at temperatures near and above  $T_C$  is poorer although still qualitatively correct. Considering the approximations involved in the theoretical expression, the agreement is considered satisfactory throughout the temperature range investigated. The need is indicated for a theoretical calculation to higher order.

### I. INTRODUCTION

THE theory of microwave magnetic resonance in the heavy rare-earth metals was first presented by Cooper *et al.*<sup>1</sup> in 1962, and was discussed in further detail by Cooper and Elliott<sup>2</sup> in 1963. (The latter reference will hereafter be referred to as CE). Since then, resonant microwave power absorption has been

studied in dysprosium, terbium, and erbium at 9 and 35 GHz by Bagguley and Liesegang,<sup>3</sup> and in dysprosium at 38 GHz by Rossol *et al.*<sup>4</sup> The latter have observed ferromagnetic resonance in Dy with the aid of an appreciable effective hexagonal anisotropy field which occurs in Dy below about 110°K. The presence of this hexagonal anisotropy field allows the resonance frequency to be brought down, by application of an ex-

\* Work performed in the Ames Laboratory of the U.S. Atomic Energy Commission. Contribution No. 1991.

† Present address: Cavendish Laboratory, Cambridge, England.

<sup>1</sup> B. R. Cooper, R. J. Elliott, S. J. Nettel, and H. Suhl, *Phys. Rev.* **127**, 57 (1962).

<sup>2</sup> B. R. Cooper and R. J. Elliott, *Phys. Rev.* **131**, 1043 (1963).

<sup>3</sup> D. M. S. Bagguley and J. Liesegang, *Phys. Letters* **17**, 96 (1965); *J. Appl. Phys.* **37**, 1220 (1966).

<sup>4</sup> F. C. Rossol, B. R. Cooper, and R. V. Jones, *J. Appl. Phys.* **36**, 1209 (1965); F. C. Rossol and R. V. Jones, *ibid.* **37**, 1227 (1966).